

# Robust Measurements of $n$ -Point Correlation Functions of Driven-Dissipative Quantum Systems on a Digital Quantum Computer

Lorenzo Del Re<sup>1,2</sup>, Brian Rost<sup>1</sup>, Michael Foss-Feig<sup>3</sup>, A. F. Kemper<sup>4</sup>, and J. K. Freericks<sup>1</sup>

<sup>1</sup>Department of Physics, Georgetown University, 37th and O Streets, NW, Washington, DC 20057, USA

<sup>2</sup>Max Planck Institute for Solid State Research, D-70569 Stuttgart, Germany

<sup>3</sup>Quantinuum, 303 S. Technology Court, Broomfield, Colorado 80021, USA

<sup>4</sup>Department of Physics, North Carolina State University, Raleigh, North Carolina 27695, USA



(Received 26 April 2022; accepted 16 January 2024; published 4 March 2024)

We propose and demonstrate a unified hierarchical method to measure  $n$ -point correlation functions that can be applied to driven, dissipative, or otherwise open or nonequilibrium quantum systems. In this method, the time evolution of the system is repeatedly interrupted by interacting an ancilla qubit with the system through a controlled operation, and measuring the ancilla immediately afterward. We discuss the robustness of this method as compared to other ancilla-based interferometric techniques (such as the Hadamard test), and highlight its advantages for near-term quantum simulations of open quantum systems. We implement the method on a quantum computer in order to measure single-particle Green's functions of a driven-dissipative fermionic system. This Letter shows that dynamical correlation functions for driven-dissipative systems can be robustly measured with near-term quantum computers.

DOI: 10.1103/PhysRevLett.132.100601

**Introduction.**—Open quantum systems, and in particular driven-dissipative systems, are among the most difficult problems to study in many-body physics, but also among the richest. The problem parameter space is vast; the bath as well as the system have their own inherent dynamics, and their interaction can be complex. Yet, in some sense there is a unification and emergent simplicity as the details often do not play a role when it comes to describing nonequilibrium steady (or periodic) states. These can be captured with a few parameters, have lost all knowledge of their history, and are stable to perturbations away from their fixed point. In other words, they are remarkably robust.

Their robustness has also recently been exploited in simulations on quantum computers, either relying on the hardware intrinsic decoherence [1–3], by implementing Kraus maps and Lindblad operators [4–14], or by implementing non-Hermitian dynamics [15,16]. In some cases, the existence of a fixed point has enabled quantum computers to perform the simulations far beyond the short coherence time of the qubits when the fidelity of one Trotter step is sufficiently high. It thus appears that driven-dissipative systems are promising problems for applications of near-term quantum computers.

Given this situation, it is critical to develop the tools and methodology to be able to interrogate these long-lived nonequilibrium states. For single-time operators this is not a problem, one simply measures the desired operator at some point during the evolution. However, there is a wide class of observables—correlation functions—that are of equal or greater importance as they describe the excitations of the system, and make a direct connection to experimental

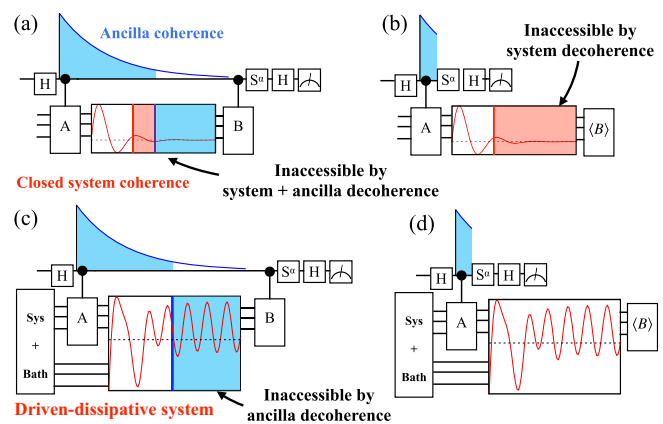


FIG. 1. Overview of the proposed new method and its region of applicability. Ancilla decoherence (blue) limits the region where the Hadamard test method (a),(c) yields a result, whereas the reset-based method (b),(d) has no such limitation. For closed system evolution (a),(b) the system decoherence naturally limits the maximal time of interest, but for driven-dissipative systems (c),(d) the reset method is necessary to go beyond the ancilla coherence time.

Published by the American Physical Society under the terms of the Creative Commons Attribution 4.0 International license. Further distribution of this work must maintain attribution to the author(s) and the published article's title, journal citation, and DOI. Open access publication funded by the Max Planck Society.

observables. The problem is that the typical protocols for the measurement of correlation functions [17–22] are based on the Hadamard test [23] [see Fig. 1(a)], where the correlation function is measured with an ancilla qubit [19,24–29].

This approach does not robustly generalize to measuring correlation functions in open quantum systems, and we illustrate the issues with it in Fig. 1 for a two-point correlation function. In short, the ancilla cannot capture the potentially long-time dynamics of the driven-dissipative open quantum systems because the ancilla has a short coherence time. For simulating closed quantum systems [Fig. 1(a)] this is not a problem because the system has an equally short coherence time, and the region of inaccessibility by the Hadamard test approach has no information. On the other hand, for simulating open quantum systems [Fig. 1(c)], this is a problem because the now-stable dynamics of the driven-dissipative system are inaccessible due to the ancilla decoherence.

In this Letter, we propose a strategy that (i) is a full framework for computing  $n$ -point correlation functions in open quantum systems, and (ii) is suitable for the near term where we cannot rely on long ancilla coherence lifetimes. Its crux is a measurement of the ancilla right after it is entangled with the system, and using the result of the measurement in postprocessing to construct the desired  $n$ -point correlation function. We illustrate the idea in Figs. 1(b) and 1(d). For simulating closed quantum systems this approach yields the same information as the standard Hadamard test; however, for open quantum systems the region of inaccessibility by ancilla decoherence is now fully accessible.

Our method is a simple strategy capable of measuring arbitrary unequal-time correlation functions between multi-qubit Pauli operators, and which works for both dissipative and unitary time evolution. As such, it subsumes and unifies the approaches of Ref. [30] (unequal-time commutators) and Ref. [31] (unequal-time anticommutators). It is hierarchical in the sense that extracting the information of an  $n$ th order correlation function requires previous knowledge of lower-order correlation functions, but it restores the robust nature of driven-dissipative systems because it does not require system-ancilla entanglement to be maintained during the time evolution of the system. We verify the validity of our method by performing measurements of the single-particle Green's function of a driven-dissipative fermionic model using a Quantinuum quantum computer. Our results show excellent quantitative agreement between data and the theoretical predictions.

*Target quantities.*—Our goal is the calculation of correlation functions of a generic system ( $S$ ) that can also dissipate energy through an interaction with a bath ( $E$ ); so we employ the density matrix formalism, which is required to study open quantum systems [32].

The correlation functions are constructed as follows. Let  $\{O_i\}$  be a set of operators in the Schrödinger representation

acting on the system Hilbert space with  $i = 1, 2, \dots, n$ , and let  $\{t_i\}$  being a set of ordered time values such that  $t_0 < t_1 < t_2 < \dots < t_{n-1} < t_n$ , where  $t_0$  is the initial time, then we define the  $n$ th rank correlation function via

$$\begin{aligned} & \langle O_n(t_n) O_{n-1}(t_{n-1}) \dots O_1(t_1) \rangle \\ & = \text{Tr}_S \{ O_n \mathcal{V}_{t_n, t_{n-1}} \dots O_2 \mathcal{V}_{t_2, t_1} O_1 \mathcal{V}_{t_1, t_0} \rho(t_0) \}. \end{aligned} \quad (1)$$

Here,  $O_i(t_i)$  is the operator  $O_i$  in the Heisenberg representation,  $\rho(t_0)$  is the system density matrix evaluated at the initial time,  $\mathcal{V}_{t_{i+1}, t_i}$  is the time evolution superoperator that evolves the system from time  $t_i$  to  $t_{i+1}$  (i.e.,  $\rho(t_{i+1}) = \mathcal{V}_{t_{i+1}, t_i} \rho(t_i)$  acting from left to right), and  $\text{Tr}_S$  indicates a trace over the system subspace (meaning that the degrees of freedom of the bath have already been integrated out). For simplicity, and without loss of generality, we assume that the operators  $O_i$  are unitary and Hermitian operators; addressing this case is sufficient to demonstrate the validity of our method, because a nonunitary operator can always be expanded as a linear combination of unitaries, chosen to also be Hermitian (e.g., Pauli strings). As will be shown in the next section, the correlation function in Eq. (1) can be extracted from the Hadamard test.

The alternative strategy that we propose will naturally yield correlation functions of nested commutators and anticommutators of the form

$$\langle [O_1(t_1), [O_2(t_2), \dots [O_{n-1}(t_{n-1}), O_n(t_n)]_{\pm} \dots]_{\pm}]_{\pm} \rangle, \quad (2)$$

where  $[\dots]_{\pm}$  can be either commutators (–) or anticommutators (+), all chosen independently. The correlation function in Eq. (1) can be obtained from the one in Eq. (2) and vice versa by performing multiple measurements and then combining the different outcomes together [33]. We note that in the case of two-point functions, Eq. (1) corresponds to lesser or greater Green's functions while Eq. (2) to advanced, retarded, and Keldysh Green's functions [37], so both methods produce all the physical Green's functions needed to describe a time evolving quantum system. However, there are some limitations—for example, one cannot directly calculate out-of-time-ordered correlation functions with the circuit in Fig. 3 and we leave possible generalizations of this method to future work.

*Hadamard test for driven-dissipative systems.*—In Fig. 2, we show how the interferometry scheme proposed in Ref. [23] generalizes to compute the  $n$ -time correlator defined in Eq. (1) for an open quantum system. In order to simulate dissipative dynamics, we need a generic  $k$ -qubit ancilla register (called  $A_2$ ) that we take to be initialized into the state  $|0\rangle = |0\rangle^{\otimes k}$ . A suitable unitary operation  $\mathcal{U}_K^{t, t'}$  that entangles  $A_2$  with the system register  $S$  followed by tracing out (ignoring) the state of the ancilla register can encode the nonunitary time evolution map  $\mathcal{V}_{t, t'}$ , which can be rewritten

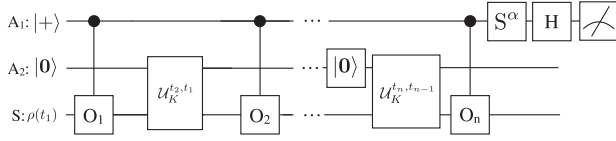


FIG. 2. The standard interferometric scheme for measuring the  $n$ -time correlation function [23], as given in Eq. (1), for a dissipative circuit. Accurate results require that the ancilla register  $A_1$  maintain coherence over the entire duration of the circuit.

using the Kraus sum representation:

$$\mathcal{V}_{t,t'}\rho(t') = \sum_{i=0}^{2^k-1} K_i(t,t')\rho(t')K_i^\dagger(t,t'), \quad (3)$$

where  $K_i$  are the so-called Kraus operators satisfying the sum rule  $\sum_i K_i^\dagger(t,t')K_i(t,t') = \mathbb{I}$ . They are related to the unitary evolution of the system and ancilla bank by  $K_i(t,t') = \langle i|U_K^{t,t'}|\mathbf{0}\rangle$ , with  $\{|i\rangle\}$  being a complete basis for  $A_2$ . In the interferometry scheme, we need an extra single-qubit ancilla register  $A_1$  in which all the information about the correlation function (which is a complex number) will be stored. For example, in the case of  $n = 2$ , the final quantum state of the  $A_1$  qubit reads

$$\rho_{A_1} = \begin{cases} \frac{1}{2}\mathbb{I}_{A_1} + \frac{1}{2}\text{Re}[C]\hat{\sigma}_{A_1}^z - \frac{1}{2}\text{Im}[C]\hat{\sigma}_{A_1}^y, & \text{if } \alpha = 0, \\ \frac{1}{2}\mathbb{I}_{A_1} - \frac{1}{2}\text{Im}[C]\hat{\sigma}_{A_1}^z - \frac{1}{2}\text{Re}[C]\hat{\sigma}_{A_1}^y, & \text{if } \alpha = 1, \end{cases} \quad (4)$$

where  $C = \langle O_2(t_2)O_1(t_1) \rangle$ , and the binary variable  $\alpha = \{0, 1\}$  indicates whether the  $S$  gate was applied or not. Measuring the ancilla in the  $Z$  and  $Y$  bases determines the real and imaginary parts of the correlation function.

This method is convenient because the complex information encoded in the correlation functions of a many-body system are found from single-qubit measurements. However, this scheme requires maintaining the coherence of the  $A_1$  ancilla (and thereby its entanglement with the system) for the full duration  $t_n - t_1$ . In the next section, we introduce an alternative robust scheme that does not require maintaining coherence of the  $A_1$  ancilla, but at the cost of requiring a more complex measurement scheme.

**Robust strategy.**—In Fig. 3, we show the alternative circuit to measure the correlation function defined in

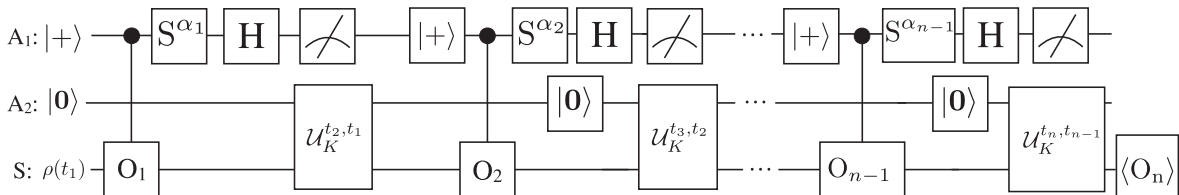


FIG. 3. Circuit to measure a generic  $n$ -time correlation function of the kind defined in Eq. (2) using the robust strategy.

Eq. (1). This circuit is schematic, because it encodes all possible circuits that are employed to measure the set of correlation functions in Eq. (2). Here, each realization has chosen unitary operations acting on  $A_1$  [selected from  $(S)^\alpha H$ , where  $S$  and  $H$  are the phase gate and the Hadamard gate, respectively] for each time  $t_i$  measured in the correlation function. The circuit shown in Fig. 3 naturally measures the set of correlation functions defined in Eq. (2) with the commutator or anticommutator chosen from the  $n - 1$  dimensional binary vector  $\alpha = \{\alpha_1, \alpha_2, \dots, \alpha_{n-1}\}$ . It is important to note that after the  $S^\alpha H$  operation is performed, the ancilla qubit  $A_1$  is measured immediately afterward and the measurement outcome ( $m_i$ ) is stored; such a measurement destroys the entanglement between  $A_1$  and the state encoded in the system and the  $A_2$  ancilla bank. The state is then evolved to the next  $t_i$  using the Kraus map decomposition defined in Eq. (3). The  $A_1$  ancilla is then reset to its  $|+\rangle$  state and the process is repeated for each operator in the correlation function. In the last step, after the final time evolution from  $t_{n-1}$  to  $t_n$ , the  $S$  register qubits will be in a final state  $\rho_n$  and the operator  $O_n$  is measured directly on the  $S$  register qubits, yielding results that depend on  $\alpha$ . The correlation function is determined by classical postprocessing of the accumulated results and the choice of  $\alpha$ .

In general, the state of the system qubits at time  $t_{j+1}$  is obtained from the state at  $t_j$  through the following map [35]:

$$\rho_{j+1} \propto \mathcal{V}_{t_{j+1},t_j}(\rho_j + O_j\rho_j O_j + [(-1)^{m_j}i^{\alpha_j}O_j\rho_j + \text{H.c.}]), \quad (5)$$

where the proportionality constant is given by tracing the rhs of the equation. Here,  $m_j = \{0, 1\}$  is the result of the  $A_1$  qubit measurement, and  $\rho_{j-1} = \rho(t_1)$  is given by the initial state of the system at time  $t_1$  (see Fig. 3).

In order to show how this method works in practice, we discuss the two simplest cases, i.e., the two-point and the three-point correlation functions. For  $n = 2$ , the result of measuring  $O_2$  directly on the system register will yield

$$\begin{aligned} \text{Tr} O_2 \rho_2 = & \mathcal{N} \{ \langle O_2(t_2) \rangle + \langle O_2(t_2) \rangle_{O_1} \\ & + \underbrace{(-1)^{m_1} [i^{\alpha_1} \langle O_2(t_2) O_1(t_1) \rangle - i^{-\alpha_1} \langle O_1(t_1) O_2(t_2) \rangle]}_{\propto \langle [O_1(t_1), O_2(t_2)]_{\mp} \rangle} \}, \end{aligned} \quad (6)$$

where  $\mathcal{N} = \{2 + [(-1)^{m_1} i^{\alpha} \langle O_1(t_1) \rangle + \text{H.c.}]\}^{-1}$ ,  $\langle O_1(t_1) O_2(t_2) \rangle = \text{Tr}(O_2 \mathcal{V}_{t_2, t_1} [\rho(t_1) O_1])$ , and  $\langle O_2(t_2) \rangle_{O_1} := \text{Tr}(O_2 \mathcal{V}_{t_2, t_1} [O_1 \rho(t_1) O_1])$ . Hence, when  $\alpha_1 = 0, 1$  the term in square brackets in Eq. (6) is proportional to  $\langle [O_1(t_1), O_2(t_2)]_{\mp} \rangle$ . This is precisely Eq. (2) when  $n = 2$ . In order to isolate our target quantity, i.e., the two-time correlation function  $\langle [O_1(t_1), O_2(t_2)]_{\mp} \rangle$ , we need to subtract the first two terms in Eq. (6) multiplied by  $\mathcal{N}$ , which are determined by equal-time averages that can be obtained by performing a set of simple extra measurements [35]. It is worthwhile to note that the measurement outcome of the ancilla  $m_1 = 0, 1$  must be stored for extracting our target quantity.

For  $n = 3$ , measuring  $O_3$  results in the following quantity:

$$\text{Tr} O_3 \rho_3 = (-1)^{m_1 + m_2} C_{t_1, t_2, t_3}^{\alpha} + R_{\alpha}, \quad (7)$$

where  $C_{t_1, t_2, t_3}^{\alpha}$  is a three-time correlation function that depends on the values of  $\alpha$ . There are four possible values:  $\langle [O_1(t_1), [O_2(t_2), O_3(t_3)]_{\pm}]_{\pm} \rangle$ . In addition, there are contributions denoted by  $R_{\alpha}$ , which is a remainder function. It is determined by performing additional measurements comparable to what is needed for lower-rank correlation functions (see Supplemental Material for details [35]).

We note that in the case of single-qubit [30,31,38] and two-qubit [39] correlators, there are alternative ways of measuring correlation functions that do not require the extra ancilla register  $A_1$ , at the cost of performing more measurements on the system [35].

**Hardware implementation.**—In order to verify the validity of the protocol, we applied it to measure the Green's function of spinless free fermions in a lattice driven by a constant electric field that also dissipate energy through a coupling with a thermal bath. The Hamiltonian of this chosen system plus bath can be brought into a block-diagonal form after performing a Fourier transform to momentum space as described in Ref. [7]. Hence, the system's reduced density matrix factorizes as a tensor product in momentum space, i.e.,  $\otimes_k \rho_k$ , and we can define a (diagonal in  $k$ ) master equation for each  $2 \times 2$   $k$ -dependent density matrix  $\rho_k$ ,

$$\partial_t \rho_k = -i[\mathcal{H}_k(t), \rho_k] + \sum_{\ell=\{1,2\}} L_{\ell} \rho_k L_{\ell}^{\dagger} - \{\rho_k, L_{\ell}^{\dagger} L_{\ell}\}, \quad (8)$$

where the Lindblad operators are  $L_1 = \sqrt{\Gamma n_F[\epsilon_k(t)]} d_k$  and  $L_2 = \sqrt{\Gamma n_F[-\epsilon_k(t)]} d_k^{\dagger}$ , with  $d_k$  being the destruction operator of a lattice fermion with quasimomentum  $k$ ,  $\epsilon_k(t) = -2J \cos(k + \Omega t)$ , with  $J$  being the hopping amplitude,  $\Omega$  the amplitude of the applied dc field, and  $k$  the crystalline momentum.  $\Gamma$  sets the strength of the system-environment coupling and  $n_F(x) = [1 + \exp(\beta x)]^{-1}$  is the Fermi-Dirac distribution with  $\beta$  being the inverse of the bath temperature. In Fig. 4, we show the circuit implementing  $\mathcal{U}_K$  for the Kraus map related to Eq. (8). The Lindblad operator

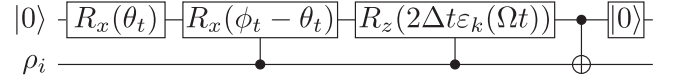


FIG. 4. Circuit implementing the Trotterized time evolution  $\mathcal{U}_K(t, t + \Delta t)$  of the model defined in Eq. (8).

$L_{1(2)}$  encodes the physical process of a Bloch electron (hole) with momentum  $k$  to hop from the lattice to the bath with a probability given by  $\Gamma n_F[-\epsilon_k(t)]$  ( $\Gamma n_F[\epsilon_k(t)]$ ). Such a decay process introduces a time dependence of the momentum distribution function of fermions and a damping of Bloch oscillations that eventually leads to a nonzero average of the dc current [7,10,35,40].

In Fig. 5, we show the retarded fermion Green's function  $G_k^{(R)}(t, t') = -i\theta(t - t') \langle [d_k(t), d_k^{\dagger}(t')]_{+} \rangle$  measured on Quantinuum's model H1-2 quantum computer. The

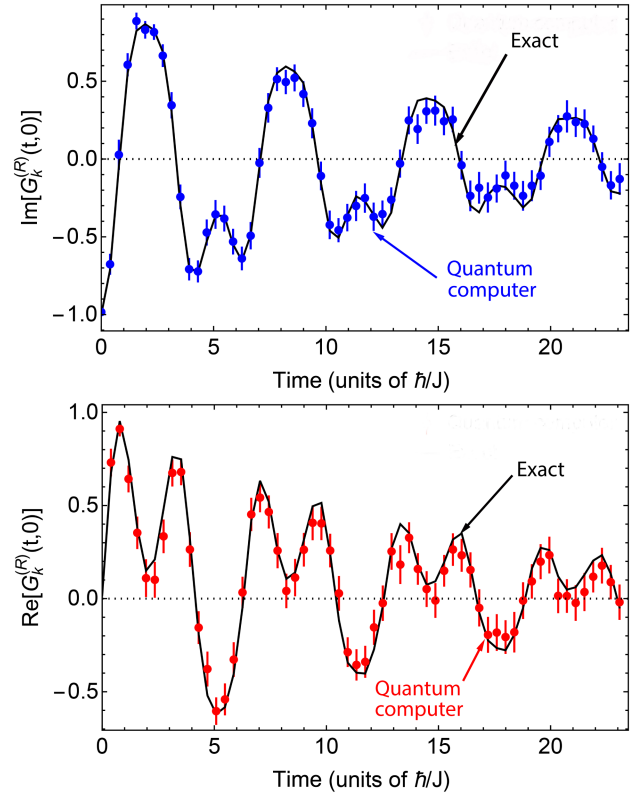


FIG. 5. Imaginary (upper panel) and real (lower panel) parts of the retarded fermion Green's function as a function of time (parameters are wave vector  $k = -0.5/a_0$  where  $a_0$  is the lattice constant, dimensionless electric field is  $\Omega = 1$ , the dissipation rate to the fermionic bath is  $\Gamma = 1/16$ , and the bath temperature is 0.01 in units of the hopping). Circles represent data from a Quantinuum model H1-2 quantum computer, with error bars representing  $2\sigma$  confidence intervals. The primary source of error in the implemented circuits is due to noise on the two-qubit gates  $[(2 - 3) \times 10^{-3}$  average infidelity]. However, the resulting noise model leads to results that are barely distinguishable by eye from exact circuit simulations (black lines) and are omitted from the figure.

retarded Green's function of the model can be computed exactly and its derivation and analytical form are given in the Supplemental Material [35].

There is excellent quantitative agreement between the data produced by the quantum computer and the expected curves in presence of noise. It is worthwhile to note that in the presence of a driving field, the Green's function does not oscillate as a simple sinusoidal function and it presents extra features, such as the additional maxima and minima occurring between time 10 and time 19 [see Fig. 5], that are faithfully reproduced by the quantum computer data.

*Conclusion and outlook.*—We have put forward a robust technique for the measurement of multipoint correlation functions of driven-dissipative quantum systems that can be applied in the realm of quantum simulations of complex models such as the Hubbard model. Unlike the Hadamard test, which requires us to keep the ancilla and system qubits coherently entangled, our new approach does not. This is advantageous for driven-dissipative systems, where the system is not coherent (see Fig. 1), although it comes at the cost of performing extra measurements, as well as requiring additional circuits of lower depth than the one needed to extract the target quantity. Our method naturally computes correlators of the form given in Eq. (2), which represent a myriad of response functions and experimental measurements. We applied our method to measuring the Green's function of free fermions driven out of equilibrium and interacting with a bath. The data obtained from the quantum computer are in an excellent agreement with the curves predicted by the theory. While these data constitute an important proof of principle enabling the measurement of correlation functions on near-term quantum computers, further work needs to be done to use this approach to solve new problems in science.

Interestingly, given its generality, the Hadamard test has applications other than the measurement of correlation functions; for example, it has been proposed for determining important overlaps in the realm of variational quantum dynamics simulations [41,42] and also for the simulation of open quantum systems using quantum imaginary-time evolution [13]. We therefore expect our robust alternative strategy to the Hadamard test to be suitable for these other applications as well.

We acknowledge financial support from the U.S. Department of Energy, Office of Science, Basic Energy Sciences, Division of Materials Sciences and Engineering. Initial submission and project execution were performed under Grant No. DE-SC0019469; the resubmission under Grant No. DE-SC0023231. B. R. was also funded by the National Science Foundation under Grant No. DMR-1747426 (QISE-NET). J. K. F. was also funded by the McDevitt bequest at Georgetown University.

- [1] C. H. Tseng, S. Somaroo, Y. Sharf, E. Knill, R. Laflamme, T. F. Havel, and D. G. Cory, Quantum simulation with natural decoherence, *Phys. Rev. A* **62**, 032309 (2000).
- [2] B. Rost, B. Jones, M. Vyushkova, A. Ali, C. Cullip, A. Vyushkov, and J. Nabrzyski, Simulation of thermal relaxation in spin chemistry systems on a quantum computer using inherent qubit decoherence, [arXiv:2001.00794](https://arxiv.org/abs/2001.00794).
- [3] O. E. Sommer, F. Piazza, and D. J. Luitz, Many-body hierarchy of dissipative timescales in a quantum computer, *Phys. Rev. Res.* **3**, 023190 (2021).
- [4] J. T. Barreiro, M. Müller, P. Schindler, D. Nigg, T. Monz, M. Chwalla, M. Hennrich, C. F. Roos, P. Zoller, and R. Blatt, An open-system quantum simulator with trapped ions, *Nature (London)* **470**, 486 (2011).
- [5] A. M. Childs and T. Li, Efficient simulation of sparse Markovian quantum dynamics, *Quantum Inf. Comput.* **17**, 901 (2017).
- [6] R. Cleve and C. Wang, Efficient quantum algorithms for simulating lindblad evolution, [arXiv:1612.09512](https://arxiv.org/abs/1612.09512).
- [7] L. Del Re, B. Rost, A. F. Kemper, and J. K. Freericks, Driven-dissipative quantum mechanics on a lattice: Simulating a fermionic reservoir on a quantum computer, *Phys. Rev. B* **102**, 125112 (2020).
- [8] S. Tornow, W. Gehrke, and U. Helmbrecht, Non-equilibrium dynamics of a dissipative two-site Hubbard model simulated on ibm quantum computers, *J. Phys. A* **55**, 245302 (2022).
- [9] Z. Hu, R. Xia, and S. Kais, A quantum algorithm for evolving open quantum dynamics on quantum computing devices, *Sci. Rep.* **10**, 3301 (2020).
- [10] B. Rost, L. Del Re, N. Earnest, A. F. Kemper, B. Jones, and J. K. Freericks, Demonstrating robust simulation of driven-dissipative problems on near-term quantum computers, [arXiv:2108.01183](https://arxiv.org/abs/2108.01183).
- [11] Z. Hu, K. Head-Marsden, D. A. Mazziotti, P. Narang, and S. Kais, A general quantum algorithm for open quantum dynamics demonstrated with the Fenna-Matthews-Olson complex, *Quantum* **6**, 726 (2022).
- [12] A. W. Schlimgen, K. Head-Marsden, LeeAnn M. Sager, P. Narang, and D. A. Mazziotti, Quantum simulation of open quantum systems using a unitary decomposition of operators, *Phys. Rev. Lett.* **127**, 270503 (2021).
- [13] H. Kamakari, S.-N. Sun, M. Motta, and A. J. Minnich, Digital quantum simulation of open quantum systems using quantum imaginary-time evolution, *PRX Quantum* **3**, 010320 (2022).
- [14] M. Cattaneo, M. A. C. Rossi, G. García-Pérez, R. Zambrini, and S. Maniscalco, Quantum simulation of dissipative collective effects on noisy quantum computers, *PRX Quantum* **4**, 010324 (2023).
- [15] J. Hubisz, B. Sambasivam, and J. Unmuth-Yockey, Quantum algorithms for open lattice field theory, *Phys. Rev. A* **104**, 052420 (2021).
- [16] C. Zheng, Universal quantum simulation of single-qubit nonunitary operators using duality quantum algorithm, *Sci. Rep.* **11**, 3960 (2021).
- [17] D. Wecker, M. B. Hastings, N. Wiebe, B. K. Clark, C. Nayak, and M. Troyer, Solving strongly correlated electron models on a quantum computer, *Phys. Rev. A* **92**, 062318 (2015).

- [18] T. Keen, T. Maier, S. Johnston, and P. Lougovski, Quantum-classical simulation of two-site dynamical mean-field theory on noisy quantum hardware, *Quantum Sci. Technol.* **5**, 035001 (2020).
- [19] T. Steckmann, T. Keen, E. Kökcü, A. F. Kemper, E. F. Dumitrescu, and Y. Wang, Mapping the metal-insulator phase diagram by algebraically fast-forwarding dynamics on a cloud quantum computer, *Phys. Rev. Res.* **5**, 023198 (2023).
- [20] G. Greene-Diniz, D. Z. Manrique, K. Yamamoto, E. Plekhanov, N. Fitzpatrick, M. Krompiec, R. Sakuma, and D. M. Ramo, Quantum computed Green's functions using a cumulant expansion of the Lanczos method, [arXiv:2309.09685](https://arxiv.org/abs/2309.09685).
- [21] G. Bishop, D. Bagrets, and F. K. Wilhelm, Quantum algorithm for Green's functions measurements in the Fermi-Hubbard model, [arXiv:2310.10412](https://arxiv.org/abs/2310.10412).
- [22] D. Dhawan, D. Zgid, and M. Motta, Quantum algorithm for imaginary-time Green's function, [arXiv:2309.09914](https://arxiv.org/abs/2309.09914).
- [23] R. Somma, G. Ortiz, J. E. Gubernatis, E. Knill, and R. Laflamme, Simulating physical phenomena by quantum networks, *Phys. Rev. A* **65**, 042323 (2002).
- [24] J. M. Kreula, L. García-Álvarez, L. Lamata, S. R. Clark, E. Solano, and D. Jaksch, Few-qubit quantum-classical simulation of strongly correlated lattice fermions, *Eur. Phys. J. Quantum Technol.* **3**, 11 (2016).
- [25] J. Kreula, S. R. Clark, and D. Jaksch, Non-linear quantum-classical scheme to simulate non-equilibrium strongly correlated fermionic many-body dynamics, *Sci. Rep.* **6**, 32940 (2016).
- [26] A. Chiesa, F. Tacchino, M. Grossi, P. Santini, I. Tavernelli, D. Gerace, and S. Carretta, Quantum hardware simulating four-dimensional inelastic neutron scattering, *Nat. Phys.* **15**, 455 (2019).
- [27] A. Francis, J. K. Freericks, and A. F. Kemper, Quantum computation of magnon spectra, *Phys. Rev. B* **101**, 014411 (2020).
- [28] B. Jaderberg, A. Agarwal, K. Leonhardt, M. Kiffner, and D. Jaksch, Dynamical mean field theory algorithm and experiment on quantum computers, *Quantum Sci. Technol.* **5**, 034015 (2020).
- [29] S.-N. Sun, M. Motta, R. N. Tazhigulov, A. T. K. Tan, Garnet Kin-Lic Chan, and A. J. Minnich, Quantum computation of finite-temperature static and dynamical properties of spin systems using quantum imaginary time evolution, *PRX Quantum* **2**, 010317 (2021).
- [30] M. Knap, A. Kantian, T. Giamarchi, I. Bloch, M. D. Lukin, and E. Demler, Probing real-space and time-resolved correlation functions with many-body Ramsey interferometry, *Phys. Rev. Lett.* **111**, 147205 (2013).
- [31] P. Uhrich, S. Castrignano, H. Uys, and M. Kastner, Noninvasive measurement of dynamic correlation functions, *Phys. Rev. A* **96**, 022127 (2017).
- [32] H.-P. Breuer and F. Petruccione, *The Theory of Open Quantum Systems* (Oxford University Press, New York, on Demand, 2002).
- [33] The correlation function in Eq. (2) is not the most general  $n$ -point correlation function because it always maintains Keldysh time ordering on a two branch Keldysh contour, as opposed to the most general form, which requires higher-order Keldysh contours [34]; for concrete examples, see the Supplemental Material [35].
- [34] N. Tsuji, P. Werner, and M. Ueda, Exact out-of-time-ordered correlation functions for an interacting lattice fermion model, *Phys. Rev. A* **95**, 011601(R) (2017).
- [35] See Supplemental Material at <http://link.aps.org/supplemental/10.1103/PhysRevLett.132.100601> for additional derivations of the correlation functions, details of the quantum hardware, and resource estimates, which includes Refs. [34,36].
- [36] E. Andersson, J. D. Cresser, and M. J. W. Hall, Finding the kraus decomposition from a master equation and vice versa, *J. Mod. Opt.* **54**, 1695 (2007).
- [37] G. Stefanucci and R. van Leeuwen, *Nonequilibrium Many-Body Theory of Quantum Systems: A Modern Introduction* (Cambridge University Press, Cambridge, England, 2013).
- [38] A. Schuckert and M. Knap, Probing eigenstate thermalization in quantum simulators via fluctuation-dissipation relations, *Phys. Rev. Res.* **2**, 043315 (2020).
- [39] K. Mitarai and K. Fujii, Methodology for replacing indirect measurements with direct measurements, *Phys. Rev. Res.* **1**, 013006 (2019).
- [40] J. E. Han, Solution of electric-field-driven tight-binding lattice coupled to fermion reservoirs, *Phys. Rev. B* **87**, 085119 (2013).
- [41] X. Yuan, S. Endo, Q. Zhao, Y. Li, and S. C. Benjamin, Theory of variational quantum simulation, *Quantum* **3**, 191 (2019).
- [42] Y.-X. Yao, N. Gomes, F. Zhang, C.-Z. Wang, K.-M. Ho, T. Iadecola, and P. P. Orth, Adaptive variational quantum dynamics simulations, *PRX Quantum* **2**, 030307 (2021).